

Structural and electronic properties of semiconductor binary microclusters $A_m B_n$ ($A, B = \text{Si, Ge, C}$): A B3LYP-DFT study

Si-Dian Li,^{1,2} Zhi-Guang Zhao,² Xiu-Feng Zhao,² Hai-Shun Wu,³ and Zhi-Hao Jin¹

¹*School of Materials Science and Engineering, Xian Jiaotong University, Xian 710049, People's Republic of China*

²*Department of Chemistry, Xinzhou Teachers' University, Xinzhou 034000, Shanxi, People's Republic of China*

³*Institute of Materials Chemistry, Shanxi Normal University, Linfen 041000, Shanxi, People's Republic of China*

(Received 26 April 2001; published 15 October 2001)

Structural and electronic properties of semiconductor binary microclusters $A_m B_n$ ($A, B = \text{Si, Ge, C}$) have been investigated using the B3LYP-DFT method in the range $s = m + n \leq 10$. Full structural optimization and frequency analyses are performed with the basis of 6-311G(3df). Geometries of $A_m B_n$ binary clusters are found to follow similar structural patterns with lower symmetries when compared with corresponding elemental Si_s and Ge_s in this size range. The optimized structures have either singlet or triplet ground states, depending on specific cluster size, cluster composition, and configurations. Similar to the ionization potentials of Ge_s clusters in the same size range, the calculated vertical ionization potentials of $\text{Si}_m \text{Ge}_n$ vary with an even-odd alternation in the range of $s = 2-7$, a global minimum at $s = 8$ ($C_s \text{Si}_4 \text{Ge}_4$) and an obvious recovery at $s = 9$ ($C_{2v} \text{Si}_5 \text{Ge}_4$) and $s = 10$ ($C_{3v} \text{Si}_6 \text{Ge}_4$). Both $\text{Si}_4 \text{Ge}_6$ and $\text{Si}_6 \text{Ge}_4$ are predicted to be species with high stabilities and possible to be produced experimentally.

DOI: 10.1103/PhysRevB.64.195312

PACS number(s): 73.22.-f, 61.46.+w

I. INTRODUCTION

Structures of semiconductor microclusters of Si_n and Ge_n have been known to be quite different from those of the bulk materials, and the geometrical and electronic property transitions with increasing cluster sizes have been the focus of most theoretical and experimental studies.¹⁻⁵ Ion-drift-tube mobility measurements¹ and local density approximation (LDA) calculations^{2,3} have indicated that small-sized Si_n ($n \leq 27$) exist as prolate stacks of tricapped trigonal prism of Si_9 and germanium and tin clusters follow very similar growth pattern in small size range, but fundamentally different in medium size range. Structural transitions from prolate to bulklike spheres occur for Si_n , Ge_n , and Sn_n at different sizes with $n \approx 27$, 65, and 35, respectively.^{4,5} A comparative study of the dynamical properties of C_n , Si_n , Ge_n , and Sn_n was reported recently by Lu *et al.*⁶ We performed a B3PW91-DFT/6-311G(d) study on the ionization potentials, electron affinities and vibration frequency analyses of Ge_n neutrals and charged ions⁷ very recently. Experimental evidence and theoretical calculations have demonstrated that although silicon and germanium are similar in bulk, the 4-5% difference in atomic radii between their atoms and the increase of metallicity have introduced obviously different properties to their elemental microclusters.

It is reasonable to ask what happens for binary clusters $\text{Si}_m \text{Ge}_n$ if they can be made in experiments under certain conditions. One could anticipate that there should be interesting properties existing for binary $\text{Si}_m \text{Ge}_n$ microclusters. The structural and electron property transitions from microclusters to medium-sized clusters and to binary SiGe bulk would occur at certain sizes between those of silicon and germanium systems. SiGe technology has been studied extensively in the past ten years and the binary heterostructure $\text{Si}/\text{Si}_{1-x}\text{Ge}_x$ has produced a new generation of high performance heterojunction bipolar transistors (HBT), field effect

transistors and infrared detectors.^{8,9} Studies on binary and ternary semiconductor clusters may provide insight into the bulk alloy structures, especially in the interfacial areas where the lattice mismatch occurs due to the change of atomic composition. But as we know, there have been no electronic calculations nor experimental results reported for $\text{Si}_m \text{Ge}_n$ or $\text{Si}_m \text{C}_n$ binary microclusters so far. Li *et al.*¹⁰ performed a semiempirical nonorthogonal tight-binding study of the low-energy structures of $\text{Si}_m \text{Ge}_n$ clusters in a very recent paper, but more strict theoretical investigation is obviously needed because of the fact that averaged parameters of Si and Ge were used in the tight-binding approach designed for $\text{Si}_m \text{Ge}_n$ (Ref. 10) and frequency analysis has not been performed to check the stabilities of the optimized structures. In this work we present a density function theory study for semiconductor binary systems $A_m B_n$ with $A, B = \text{Si, Ge, C}$ and $s = m + n \leq 10$. We aim to provide more reliable ground-state geometries and electronic states, relative orbital and total energies, HOMO-LUMO gaps and theoretically calculated IR vibration frequencies at the corresponding optimum structures. A comparison with Si_n and Ge_n in the same size range would shed useful insight into the similarities and differences between the binary system and corresponding elemental clusters.

II. METHODOLOGY

The B3LYP-DFT/6-311G(3df) method has been employed to optimize the geometries of semiconductor binary systems. Frequency analyses are also performed at the same theoretical level to check whether the optimum structures are transition states or true minima on the potential energy surfaces of corresponding cluster systems. The choice of density functional theory has been fully justified for semiconductor systems studied due to the fact that it is an *ab initio* tool and it includes the electron correlation effect which has been found necessary for silicon and germanium clusters at rela-

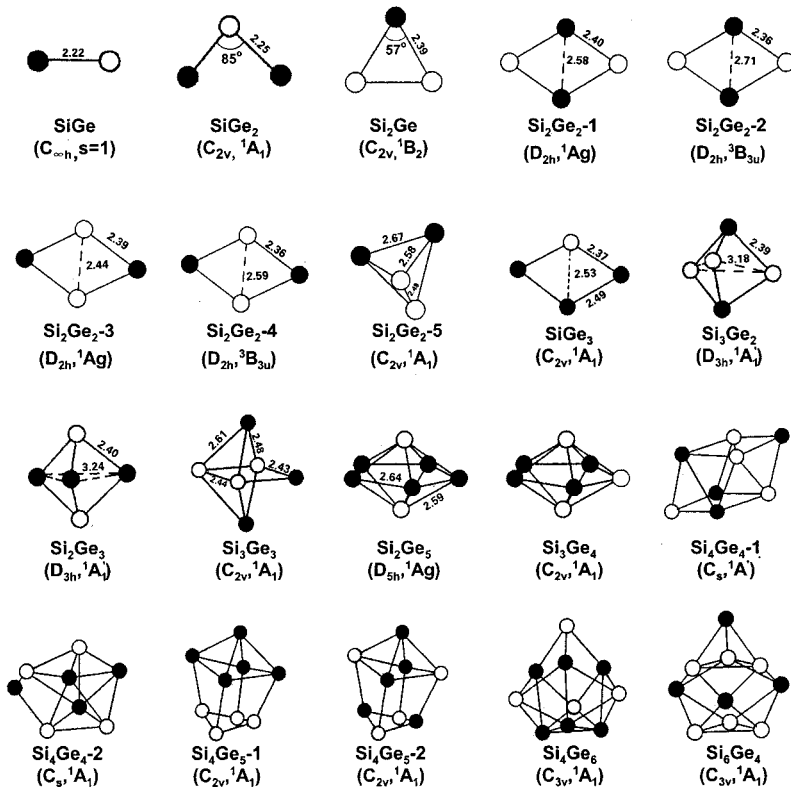


FIG. 1. Selected low-energy structures obtained for Si_mGe_n ($m+n \leq 10$). Open circles represent Si atoms and the real ones stand for Ge atoms.

tively low computational cost.¹¹ The initial input structures are taken from either references published before for Si_n and Ge_n and replace some of the atoms, or the tight-binding results reported for Si_mGe_n ,¹⁰ or arbitrarily constructed, and then fully optimized via the Bery algorithm.¹² To determine the stability of the optimized structures, harmonic vibration frequencies are further calculated with B3LYP functional.¹² Some optimized geometries, although low in energies, are found to be first order or even higher order stationary points [the saddle points in configuration space which have imaginary frequency(ies)]. For small clusters with $m+n=s \leq 4$, extensive geometry spaces are searched for both singlet and triplet ground states, while for bigger clusters only selected initial geometries with high symmetries are optimized for singlet states, limited by the huge computational task required in optimization process. All calculations were performed with the GAUSSIAN⁹⁸ code¹² on a Founder MM workstation.

III. RESULTS AND DISCUSSION

The optimized low-energy structures, electronic states, total energies, HOMO-LUMO energy gaps, and the three strongest vibration frequencies of Si_mGe_n are depicted in Fig. 1 and tabulated in Table I. For “tetramers” ($s=m+n=4$), structures with different multiplicities ($2s+1=1,3$) are also shown for Si_2Ge_2 to demonstrate the structural difference introduced by different spin occupations which will be discussed with more details later.

A. Linear AB : SiGe , SiC , and GeC

At B3LYP/6-311G(3df) level, all AB binary clusters SiC , GeC , and SiGe have triplet ground states ($C_{\infty v}, {}^3\Sigma$)

with bond lengths of 1.71, 1.80, and 2.22 Å, bond energies of 4.36, 3.83, 2.90 eV, HOMO-LUMO gaps of 1.96, 1.80, 1.36 eV, and IR frequencies of 986, 812, and 431 cm^{-1} , respectively, while their singlet states ($C_{\infty v}, {}^1\Sigma$) lie 1.17, 1.18, and 0.99 eV above corresponding triplet states, respectively. AB binary clusters have the same multiplicities as that of elemental dimers Si_2 and Ge_2 which have been confirmed in both experiments and theory.¹¹ The bond energy order of $\text{C-C}(6.22 \text{ eV}) > \text{C-Si}(4.36 \text{ eV}) > \text{Ge-C}(3.83 \text{ eV}) > \text{Si-Si}(3.08 \text{ eV}) > \text{Si-Ge}(2.90 \text{ eV}) > \text{Ge-Ge}(2.74 \text{ eV})$ at present theoretical level for dimers and the formation energies of $A-B$ bonds show approximately the bond strength in binary cluster systems. They also provide an estimation to predict the relative stabilities of different isomers of the same cluster composition. A_mB_n binary clusters with defined atomic composition should form isomers with the greatest number of relatively strong bonds and avoid the formation of weak bonds. If the energy gain could not balance the energy loss in the process of $A-A+B-B \rightarrow 2A-B+2E$, the formation of A_mB_n clusters would not be favored in energies. Qualitative prediction made for bigger binary clusters from this estimation will be discussed in detail in the following sections.

B. Triangular AB_2 : Si_2Ge , SiGe_2 , Si_2C , SiC_2 , Ge_2C , and GeC_2

For AB_2 binary clusters of group IV elements, linear structures are excluded due to the fact that they have extremely low stabilities. The theoretically optimized ground states of SiGe_2 , Si_2C , SiC_2 , Ge_2C , and GeC_2 are singlet triangular structures $C_{2v}({}^1A_1)$ with $A-B$ bond lengths of 2.25, 1.69, 1.84, 1.78, and 1.95 Å, and $B-A-B$ bond angles of 85°, 144°, 40°, 134°, and 37°, respectively, while Si_2Ge has

TABLE I. Calculated electronic energies E_t (Hartree/particle), HOMO-LUMO energy gaps E_{gap} (eV), the three strongest IR frequencies (cm^{-1}) of Si_mGe_n binary clusters ($s = m + n \leq 10$).

Si_mGe_n	structure	E_t	E_{gap}	IR frequency
SiGe		-2366.430 027	1.36	431
SiGe ₂		-4443.497 445	2.44	424(B_2) 427(A_1) 112(A_1)
Si ₂ Ge		-2655.965 798	1.90	274(B_2) 440(A_1) 243(A_1)
Si ₂ Ge ₂	Si ₂ Ge ₂ -1	-4733.033 239	2.29	386(B_{1u}) 77(B_{3u}) 180(B_{2u})
	Si ₂ Ge ₂ -2	-4733.005 346	0.77	221(B_{1u}) 141(B_{3u})
	Si ₂ Ge ₂ -3	-4733.043 295	2.46	396(B_{1u}) 180(B_{2u}) 67(B_{3u})
	Si ₂ Ge ₂ -4	-4733.006 773	0.47	339(B_{1u}) 220(B_{2u}) 133(B_{3u})
	Si ₂ Ge ₂ -5	-4732.961 354	1.49	218(A') 276(A'') 228(A')
SiGe ₃		-6520.565 924	2.39	403(B_2) 240(B_2) 342(A_1)
Si ₃ Ge ₂		-5022.551 202	3.00	361(E') 289(A_2'') 147(E')
Si ₂ Ge ₃		-6810.096 047	3.27	337(E') 311(A_2'') 154(A_1')
Si ₃ Ge ₃		-7099.632 582	3.33	339(B_1) 408(A_1) 376(A_1)
Si ₂ Ge ₅		-10 964.209 519	3.16	298(E_1') 171(A_2'') 149(E_1')
Si ₃ Ge ₄		-9176.669 565	2.79	325(A_1) 246(B_2) 321(B_2)
Si ₄ Ge ₄	Si ₄ Ge ₄ -1	-9466.164 885	2.44	426(A') 341(A'') 278(A')
	Si ₄ Ge ₄ -2	-9466.148 481	1.73	270(A'') 296(A') 447(A')
Si ₅ Ge ₄	Si ₅ Ge ₄ -1	-9755.699 248	2.76	452(A_1) 246(B_2) 387(B_1)
	Si ₅ Ge ₄ -2	-9755.684 147	2.86	380(A_1) 361(B_2) 249(B_1)
Si ₄ Ge ₆		-13 620.281 827	3.11	315(E) 356(A_1) 204(E)
Si ₆ Ge ₄		-10 045.244 565	2.74	382(E) 392(A_1) 208(A_1)

a triplet triangular C_{2v} (3B_2) ground-state geometry with Si-Ge bond length of 2.39 Å and Si-Ge-Si bond angle of 57° , a special angle very close to 60° . In comparison with elemental trimers Si_3 and Ge_3 which all have singlet ground states,¹¹ Si_2Ge is the only binary cluster which has a 3B_2 triplet ground state (lying 0.24 eV lower in energy than corresponding 1A_1 singlet state) in the six AB_2 “trimers.” It is an example showing how the composition effect plays an important role upon spin occupation. The bond angles of 57° in Si_2Ge and 85° in SiGe_2 indicate that the Si-Si interaction is stronger than Si-Ge and Si-Ge is stronger than Ge-Ge in these “trimers” (see Fig. 1), in line with bond strength order obtained above from “dimers.” It should also be pointed out that $B-A-B$ bond angles expand with the apex atoms varying from Ge, Si, to C and the end atoms from C, Si, to Ge. For example, the Ge-Si-Ge bond angle in SiGe_2 (1A_1), Si-C-Si angle in Si_2C (1A_1) and Ge-C-Ge angle in Ge_2C (1A_1) are 85° , 144° , and 134° , respectively. The triplet triangular Ge_2C (3B_1), which lies 2.45 eV above the singlet ground state, has a Ge-C-Ge bond angle of 179.9° . It is in fact a linear structure.

C. Rhombus A_2B_2 : Si_2Ge_2 , Si_2C_2 , and Ge_2C_2

Similar to Si_4 and Ge_4 , planar rhombus (D_{2h}) A_2B_2 ($A, B = \text{C, Si, Ge}$) are much more stable than both linear and tetrahedron structures. Most A_2B_2 binary clusters have D_{2h} singlet states (1A_g) as their most stable states, but for Si-Si diagonally bonded Si_2C_2 and Ge-Ge diagonally bonded Ge_2C_2 , triplet states (${}^3B_{3u}$) are more stable than corresponding singlet states (1A_g). Total energies tabulated in Table I

indicate that for Si_2Ge_2 , the rhombuses with weak Si-Si diagonal interaction (Si_2Ge_2 -3 and -4 in Fig. 1) are more stable than their isomers with direct Ge-Ge interaction (Si_2Ge_2 -1 and -2). In the four isomers, the singlet C_{2v} Si_2Ge_2 -3(1A_g), which has a Si-Si diagonal weak bond, is the ground state of Si_2Ge_2 . It is 0.27 eV lower than Si_2Ge_2 -1(1A_g), 1.03 eV lower than Si_2Ge_2 -2(3B_u) and 0.99 eV lower than Si_2Ge_2 -4(3B_u) in energies. The energy differences of 0.99 eV between Si_2Ge_2 -3(1A_g) and Si_2Ge_2 -4(3B_u) and 0.76 eV between Si_2Ge_2 -1(1A_g) and Si_2Ge_2 -2(3B_u) clearly indicate the stability and structural differences induced by different spin occupations of the same configuration. Similar phenomena happen for Si_2C_2 and Ge_2C_2 , in which C-C diagonal interaction is favored in energy over Si-Si and Ge-Ge diagonal bonding, again in agreement with the bond strength order obtained from dimers mentioned above. It should be noted that the 1A_g singlet state of rhombus Si_2C_2 with a Si-Si diagonal weak bond is a first order stationary point on the potential energy surface with an imaginary frequency of 1006 cm^{-1} (B_{3u} mode). The ${}^3B_{2g}$ triplet state of C-C diagonally bonded rhombus Si_2C_2 lies 2.32 eV above the ground state structure for the reason that the designed triplet state requires the last electron occupy a HOMO (α orbital) which is higher in energy than the LUMO (β orbital) of this structure.

D. Si_mGe_n with $m+n \geq 5$

For Si_mGe_n clusters with $s = m + n \geq 5$, there exist a great number of possible isomers with very little difference in structures and energies. Here we report selected low-energy structures, for which both Berny structural optimizations and

frequency analyses are performed. These high-stability structures are the most likely candidates existing for corresponding clusters.

Trigonal bipyramid or distorted trigonal bipyramid structures are found most stable for Si_mGe_n with $s = 5$. For Si_3Ge_2 and Si_2Ge_3 with D_{3h} high symmetries (see Fig. 1), the calculated Si-Ge bond lengths in vertical directions are 2.39 and 2.40 Å, respectively, while the horizontal bonds are broken, similar to Si_5 and Ge_5 . Extensive searches produce no other structures with lower energies for $s = 5$.

Si_3Ge_3 , similar to Si_6 and Ge_6 , takes an edge-capped distorted bipyramid (see Fig. 1) as its ground-state structure (C_{2v} , 1A_1). The edge-capping Ge atom is directly connected to two Si atoms in the four-membered horizontal plane to form more Si-Ge bonds (rather than Ge-Ge bonds) and the diagonal Si-Si weak interaction ($r_{\text{Si-Si}} = 2.74$ Å) provides further stabilization energy to this structure. This structure can also be viewed as a distorted octahedron in which the two apex Ge atoms move a little towards the Si atom in the four-membered rhombus opposite to the capping Ge atom.

When $s = m + n = 7$, e.g., Si_2Ge_5 , Si_5Ge_2 , and Si_3Ge_4 , the binary systems have bipyramid or distorted bipyramid structures, while all the other structures are much less stable. Two typical bipyramid structures, a D_{5h} Si_5Ge_2 and a C_{2v} Si_3Ge_4 are shown in Fig. 1. Two isomeric structures were obtained for Si_4Ge_4 , the Cs structure (Si_4Ge_4-1) deduced from the C_{2h} Ge_8 (Refs. 6 and 7) and the Cs face-capped pentagonal bipyramid (Si_4Ge_4-2), with the former lying 0.45 eV lower in energy than the latter, similar to the C_{2h} Ge_8 and Si_8 . The adjacent face bicapped octahedron Si_4Ge_4 (C_{2v}) is confirmed to be a second-order stationary point with two imaginary vibration frequencies at $248i$ (b_2) and $239i$ (b_1), respectively. The C_{2v} Bernal structure (a distorted pentagon bicapped in vertical direction) (Refs. 7 and 13) is maintained for Si_5Ge_4 . Two C_{2v} isomeric structures are shown in Fig. 1 for Si_5Ge_4 , with Si_5Ge_4-1 more stable than Si_5Ge_4-2 for the reason that the former offers more Si-Si bonds than the latter (which has more Si-Ge bonds). But for Si_4Ge_5 , Bernal C_{2v} geometry is unstable with one imaginary frequency at about 20 cm^{-1} . The tetracapped trigonal prism (C_{3v} symmetry, as shown in Fig. 1) is the most stable structure for both Si_4Ge_6 and Si_6Ge_4 . It should be noted that the two C_{3v} structures are different in bonding details with the former having a trigonal prism Ge_6 core bonded together in vertical direction, while the Si_6 prism core in the latter is broken in vertical directions basically due to the existence of four large capping Ge atoms which exert expanding forces upon the four capped four-membered silicon planes. The C_{4v} bicapped tetragonal antiprism Si_5Ge_5 is found to be a second order stationary point on the potential energy surface with one doubly degenerate imaginary frequency at $62i \text{ cm}^{-1}$ (e). Its analog, the C_2 bicapped antiprism Si_5Ge_5 with even atomic distribution, is also a second-order stationary point.

Variation of the calculated vertical ionization potentials (VIP's) of Si_mGe_n binary clusters with cluster size s is shown in Fig. 2(a) and compared with the ionization potentials of corresponding Ge_s ($s = m + n$) in Fig. 2(b). The variation of

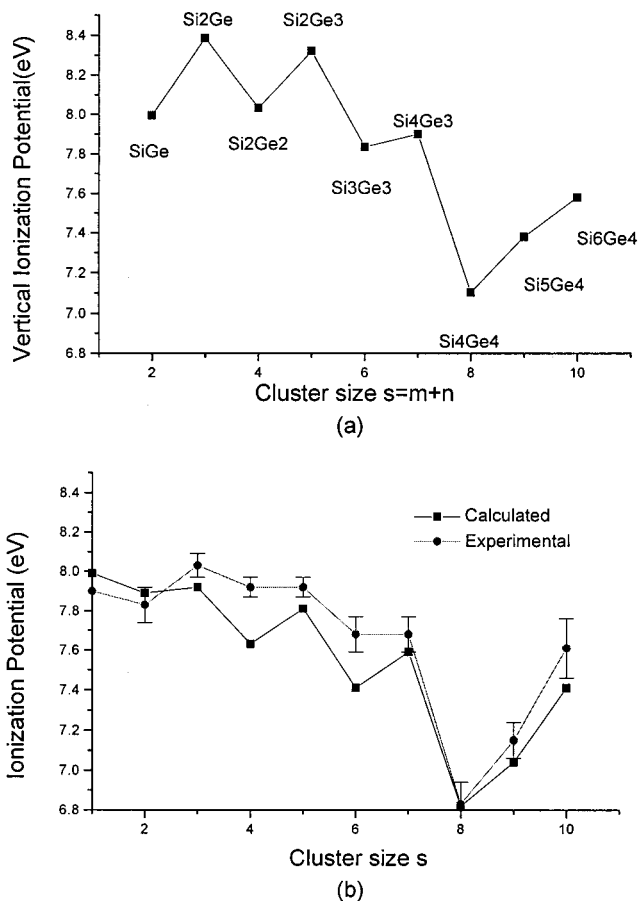


FIG. 2. Variation of the vertical ionization potentials of Si_mGe_n (a) compared with that of the experimental and calculated ionization potential of Ge_n microclusters (b).⁷

VIP's shows an even-odd alternation in the range of $s = 2 - 7$, a global minimum at $s = 8$ (7.10 eV for Si_4Ge_4), and a recovery between $s = 9$ (7.38 eV for Si_5Ge_4) and $s = 10$ (7.58 eV for Si_6Ge_4). This prediction reveals a similar ionization-potential variation between Si_mGe_n and Ge_s , for which a deep bottom at $s = 8$ and a recovery between $s = 9$ and $s = 10$ are already observed in both experiments and theory.⁷ Adiabatic ionization potentials (AIP) usually follow similar variation pattern to VIP, but with smaller values due to the energy compensation made by atomic relaxations after charging. From the variation of VIP's of Si_mGe_n , one can predict that, similar to Si_{10} and Ge_{10} , C_{3v} Si_4Ge_6 and Si_6Ge_4 are special species with high stabilities in Si_mGe_n cluster series and possible to be produced experimentally.

IV. SUMMARY

We present in this work a theoretical study of semiconductor binary clusters A_mB_n ($A = \text{Si, Ge, C}$; $s = m + n \leq 10$) using DFT-B3LYP/6-311G(3df) method. Binary clusters are found to have similar ground-state structures to corresponding elemental clusters of Si_s and Ge_s , but with more isomeric structures and lower symmetries. The ground-state structures are the ones which possess the biggest number of

stronger bonds and their spin multiplicities depend on cluster size, cluster composition, and configuration. The predicted ionization potentials of binary clusters, which are featured with the deep bottom at $s=8$ and a recovery at $s=9$ and 10 , are similar to that of Ge_s elemental clusters. Results obtained in this work present a foundation for future theoretical and

experimental study of group IV binary clusters. Further research on medium-sized A_mB_n ($s=m+n=11-50$) binary clusters is in progress. We believe that, in medium size range, more obvious structural and electronic property differences compared to elemental clusters would be observed and transitions to bulklike spherical structures would occur.

-
- ¹M. F. Jarrod and V. A. Constant, *Phys. Rev. Lett.* **67**, 2994 (1991).
- ²B. Liu, Z. Y. Lu, B. Pan, C. Z. Wang, and K. M. Ho, *J. Chem. Phys.* **109**, 9401 (1998).
- ³K. M. Ho, A. A. Shvartsburg, B. Pan, Z. Y. Lu, C. Z. Wang, J. G. Wacker, J. L. Fye, and M. F. Jarrod, *Nature (London)* **392**, 582 (1998).
- ⁴J. M. Hunter, J. L. Fye, and M. F. Jarrod, *Phys. Rev. Lett.* **73**, 2063 (1994).
- ⁵A. A. Shvartsberg and M. F. Jarrod, *Phys. Rev. A* **60**, 1235 (1999).
- ⁶Zhong-Yi Lu, Cai-Zhuang Wang, and Kai-ming Ho, *Phys. Rev. B* **61**, 2329 (2000).
- ⁷Sidian Li, Haishun Wu, and Zhihao Jin, *J. Chem. Phys.* (to be published).
- ⁸C. K. Maiti, L. K. Bera, S. Maikap, S. K. Ray, and N. B. Chakrabarti, *Def. Sci. J.* **50**, 299 (2000).
- ⁹D. De Salvador, M. Petrovich, M. Berti, F. Romanato, E. Napolitani, A. Drigo, J. Stangl, S. Zerlauth, M. Muhlberger, F. Schaffler, G. Bauer, and P. C. Kelires, *Phys. Rev. B* **61**, 13 005 (2000).
- ¹⁰Sidian Li and Zhihao Jin, *Chem. J. Chin. Universities* **21**, 1468 (2000).
- ¹¹E. F. Archibong and A. At-Amant, *J. Chem. Phys.* **109**, 962 (1998).
- ¹²M. J. Frisch, G. W. Trucks, H. B. Schlegel, G. E. Scuseria, M. A. Robb, J. R. Cheeseman, V. G. Zakrzewski, J. A. Montgomery, Jr., R. E. Stratmann, J. C. Burant, S. Dapprich, J. M. Millam, A. D. Daniels, K. N. Kudin, M. C. Strain, O. Farkas, J. Tomasi, V. Barone, M. Cossi, R. Cammi, B. Mennucci, C. Pomelli, C. Adamo, S. Clifford, J. Ochterski, G. A. Petersson, P. Y. Ayala, Q. Cui, K. Morokuma, D. K. Malick, A. D. Rabuck, K. Raghavachari, J. B. Foresman, J. Cioslowski, J. V. Ortiz, B. B. Stefanov, G. Liu, A. Liashenko, P. Piskorz, I. Komaromi, R. Gomperts, R. L. Martin, D. J. Fox, T. Keith, M. A. Al-Laham, C. Y. Peng, A. Nanayakkara, G. Gonzalez, M. Challacombe, P. M. W. Gill, B. Johnson, W. Chen, M. W. Wong, J. L. Andres, C. Gonzalez, M. Head-Gordon, E. S. Replogle, and J. A. Pople, *GAUSSIAN 98, Revision A.6*, Gaussian, Inc., Pittsburgh, PA, 1998.
- ¹³S. Ogut and J. R. Chelikowsky, *Phys. Rev. B* **55**, R4914 (1997).